NASA TECHNICAL NOTE

NASA TN D-2401

NASA TN D-2401

EXPERIMENTAL INVESTIGATION OF HEAVY-MOLECULE PROPELLANTS IN AN ELECTRON-BOMBARDMENT THRUSTOR

by David C. Byers, William R. Kerslake, and Jack Grobman

Lewis Research Center
Cleveland, Ohio

NATIONAL AERONAUTICS AND SPACE ADMINISTRATION • WASHINGTON, D. C. • AUGUST 1964

EXPERIMENTAL INVESTIGATION OF HEAVY-MOLECULE PROPELLANTS IN AN ELECTRON-BOMBARDMENT THRUSTOR

By David C. Byers, William R. Kerslake, and Jack Grobman

Lewis Research Center
Cleveland, Ohio

NATIONAL AERONAUTICS AND SPACE ADMINISTRATION

For sale by the Office of Technical Services, Department of Commerce,
Washington, D.C. 20230 -- Price $1.00

EXPERIMENTAL INVESTIGATION OF HEAVY-MOLECULE PROPELLANTS IN AN ELECTRON-BOMBARDMENT THRUSTOR

by David C. Byers, William R. Kerslake, and Jack Grobman

Lewis Research Center

SUMMARY

An experimental program was undertaken to determine the performance of several heavy molecular compounds in a 10-centimeter-diameter electron-bombardment ion thrustor. The effects of various thrustor parametric changes on the overall performance of a particular heavy molecular compound were also investigated.

The experimental results indicated that heavy-molecule ion beams could not be produced in quantity, at acceptable levels of thrustor efficiency, from an electron-bombardment thrustor of a design presently used with monatomic propellants. The study of the performance of several test molecular propellants suggested that thrustor discharge phenomena were more important in determining the average mass of the ions in the exhaust beam than were molecular composition and structural characteristics. Variation of a number of thrustor parameters in an attempt to reduce molecular fragmentation produced no significant improvement in overall thrustor performance.

INTRODUCTION

An experimental program was initiated to investigate the feasibility of employing high-molecular-weight compounds as propellants in an electron-bombardment thrustor. The desire for using heavy molecules, (i.e., with masses greater than 200 amu) arises primarily from the fact that, at a given specific impulse, the thrustor power efficiency would be expected to increase as ion mass to charge ratio is increased, provided that the energy required to form an ion does not vary significantly with ion mass. This effect is of particular interest at specific impulses below 10,000 seconds (ref. 1). The use of heavy molecules would result in larger accelerator grid spacings as a consequence of the practical limit on electric field intensities between the accelerator grids (ref. 2). This increased spacing should ease practical design and fabrication problems for thrustors operating in the specific impulse range of interest.

The study herein consisted of two phases. First, an attempt was made to determine the performance of the test propellants in a 10-centimeter-diameter thrustor. For this phase, most of the molecules were selected on the basis of stability to electron impact (ref. 3) and high vapor pressure at moderate temperatures. Thrust target measurements were taken over a variety of thrustor operating conditions in order to determine the effective mass of the ions in the thrustor ion beam. Operational data, such as propellant utilization efficiency and thrustor power efficiency, were computed throughout the tests.

In the second phase, a program of variation of geometric and electrical thrustor parameters was undertaken in order to determine which physical phenomena are most responsible for fragmentation. Possible processes might include fragmentation due to wall interactions, excessive propellant temperature, excessive primary electron energy, multiple impact, and apparent fragmentation due to multiple ionization. Most data in this phase were taken with stannic iodide as a propellant.

APPARATUS AND PROCEDURE

A cutaway sketch of the 10-centimeter-diameter electron-bombardment thrustor used for the bulk of the experiments and on which most modifications were made is shown in figure 1. A schematic diagram of the electrical system is shown in figure 2.

The propellant flows through a calibrated orifice between the vaporizer and the flow distributor. After leaving the distributor, the flow enters the ion chamber. A field winding surrounding the ion chamber provides a magnetic field roughly parallel to the axis of the ion chamber. Electrons from a hot filament bombard the neutral molecules in the ion chamber, ionizing some of them. The ions then diffuse to the ion-accelerating region between the screen and accelerator plate and are ejected from the thrustor. The performance of this type thrustor with mercury as a propellant has been described previously (ref. 4).

External electrical circuitry provided control over the thrustor discharge and output parameters. The primary electron energy is essentially a function of the ion-chamber potential difference (discharge voltage). The level of ion beam current is, in general, proportional to the filament emission current, although the exact dependence is strongly affected by the other thrustor variables. The interrelation of the various thrustor parameters is quite complicated and is described in detail in reference 5.

Both steam-jacketed and electrically heated vaporizers (ref. 6) were used in the program. The vaporizer operating temperature and flow-limiting orifice size were chosen to produce a vapor pressure of approximately 100 to 500 microns of mercury in the vaporizer and equivalent neutral beam current J_n of about 0.15 ampere, with the assumption of a unit charge on each molecule. (All symbols are defined in appendix A.) This propellant flow rate was selected because a previous investigation (ref. 7) has shown that for an accelerator life of about 10,000 hours, with mercury propellant in a 10-centimeter-diameter

thrustor, beam currents should be about 0.15 ampere.

For those molecules for which vapor pressure data were not available, an initial calibration was made to determine the vaporizer temperature and orifice sizes necessary to produce a desired propellant flow rate. With a known vaporizer temperature, orifice size, and mass flow rate (from weight loss over a known time period) it was possible to estimate the vapor pressure (e.g., ref. 8). Experimental data on the test molecules are listed in table I.

As the flow calibration gave only approximate results, the propellant mass was weighed before and after each thrustor run to determine the integrated neutral flow rate. The length of a typical thrustor test was longer than 1 hour, and as the temperature would remain constant to within $1/2^{\circ}$ C with steam vaporizers, a good estimate of the average neutral propellant flow rate could be obtained. Steam-jacketed vaporizers provided more accurate temperature control than the electric vaporizer and hence were utilized whenever possible.

The investigation was conducted in one of the 5-foot-diameter 16-foot-long vacuum facilities at the NASA Lewis Research Center. The tank, shown in figure 3, has three 32-inch oil-diffusion pumps that feed into a common ejector pump, followed by a mechanical pump. With cryogenic pumping used in conjunction with the pumps, tank pressures of approximately 10^{-6} millimeter of mercury were maintained during thrustor operation.

Thrust Measurement

The thrust of the ion beam was measured with conical thrust targets, which were all 50 centimeters long and either 25 or 28 centimeters wide at the base and were fabricated of 0.025-millimeter-thick stainless steel or 0.05-millimeter-thick titanium. Titanium was found preferable primarily because of its light weight. Titanium is also advantageous because of its low sputtering yield (ref. 9) and ability to withstand high temperatures.

Figure 3 also shows the location of the thrust target (similar in construction to that described in ref. 10) and the thrustor. The distance between the thrustor and the thrust target was 40 centimeters.

During operation of the thrustor, the target was deflected by the ion beam. If the thrust and the ion beam parameters are known, it is possible to calculate the effective mass of the impinging beam particles from the equation

$$F = C\sqrt{V_I}\, J_B \sqrt{M_m} \tag{1}$$

where F is the measured thrust in newtons, C is a constant, V_I is the anode potential in volts, J_B is the beam current in amperes, and M_m is the effective ion mass in atomic mass units.

Appendix B gives a more complete description of the thrust measuring device, the methods of calibration, the significance of the thrust target

measurement, and an evaluation of the experimental accuracy of the device, which is estimated to be ±20 percent in determining M_m.

The propellant utilization efficiency was calculated from the product

$$\eta_u = \frac{J_B}{J_n} \frac{M_m}{M_p} \tag{2}$$

where J_n is the neutral beam current and M_p is the parent ion mass.

Possible Modes of Molecular Fragmentation

While an electron-bombardment thrustor can produce large beams of parent ions when atomic species are utilized as propellants, the use of molecular compounds might lead to considerable fragmentation in the thrustor discharge (ref. 3). If even a small fraction of the propellant should be converted to ions of low mass to charge ratio, either by fragmentation or multiple ionization, the potential advantages arising from the use of heavy molecules would soon disappear. It is therefore of interest to consider the possible processes that might give rise to such species. Five such processes will be considered: wall interactions, fragmentation due to excessive neutral propellant temperature, fragmentation by primary electrons, multiple impact by primary electrons, and multiple ionization.

Wall interactions. - Impact of ions on the walls of the ionization chamber was considered as a possible cause of molecular ion fragmentation. Reference 4 indicates that there is a considerable mercury ion current to the chamber surfaces from the plasma in the ionization chamber. The approximate magnitude of this ion current is deduced from electron currents in external circuitry and from the increased energy required to form each beam ion as the ionization chamber length is increased.

Because the bulk of the plasma is within a few volts of the anode potential (ref. 11), ions could fall to the screen, the filament, and the distributor plate with energies of the order of the ion-chamber potential difference. Ions formed in the anode sheath could also strike the anode with energies of a few volts (ref. 11).

Since the bond energies between atoms in a large molecule are of the order of 2 to 5 electron volts (ref. 12), such impacts might provide a mechanism for fragmentation if some of the ion kinetic energy becomes localized in a particular molecular bond.

Chemical interactions between wall surfaces and both ions and molecules could also occur (refs. 3 and 13). Evaluation of such interactions could not be made, however, without data on the specific molecule-surface system involved.

Neutral propellant temperature. - Neutrals in the discharge will probably have temperatures that are at least as high as those of the metal surfaces of

the ionization chamber, which are typically 500° K (ref. 10). Neutral temperatures of this order might contribute to molecular fragmentation. The electron-impact-fragmentation spectra of some molecules, especially the parent mass fractions, have been found experimentally to be strongly dependent on the temperature. As shown in reference 14, the parent mass fraction decreased very rapidly with temperature for some alkanes and cycloalkanes; however, the distribution of fragment ions is affected to a lesser extent. It was also found that the adverse effect of temperature increases with increasing structural complexity of the organic molecules tested.

In the ion-chamber plasma, the molecules would undergo collisions with both thermal and primary electrons, and to a much smaller extent, with ions and other molecules. Such collisions would probably determine the internal vibrational energy of the neutrals. The effects of these collisions on the molecules utilized in the program and the temperature dependence of the mass spectra of these molecules are unknown. These considerations preclude conclusions as to the consequences of such collisional processes in the discharge.

Pyrolysis (or dissociation due to excessive internal energy) in the gaseous state probably would not play a major role in determining the ultimate ion spectra in a thrustor at normal operating conditions. Even if the neutral temperature is assumed to be that of the filament, typically 2400° K (ref. 15), the internal energy, which could be localized in a particular intermolecular bond, would be small compared with the intermolecular bond strengths (ref. 12).

Primary electron impact. - It has been found for many organic molecules that the parent mass fraction, or ratio of parent to total ions, decreases very rapidly as the energy of the ionizing electron increases to approximately twice the ionization potential. At higher electron energies, the parent mass fraction remains fairly constant. Reference 14 shows the parent mass fraction as a function of electron energies for a number of organic molecules; reference 16 shows the fragmentation patterns for some of the molecules used in this program. These data, however, were taken in a mass spectrometer rather than in an electron-bombardment thrustor.

These references show also that, at energies near the ionization potential, the ionization efficiencies are quite low and increase very rapidly with increasing electron energy. For example, for 1,2,4,5-tetrabromobenzene (ionization potential, 10.7 v) the ionization efficiency increased by a factor of 7 as the ionizing electron energy increased from 14 to 20 volts.

Such data demonstrate that, to maximize the parent mass fraction, the thrustor should be operated at a discharge voltage near the ionization potential of the molecule being utilized, although considerations of ionization efficiencies indicate that the most efficient thrustor operation might be obtained at somewhat higher discharge voltages.

Multiple impact. - A calculation from reference 3 indicates that a molecule might undergo as many as 200 inelastic collisions with primary electrons before being diffused and/or accelerated from the ionization chamber. These multiple collisions might explain, in part, the discrepancies between effective ion masses calculated from data taken with a mass spectrometer and those

evaluated from the thrust of an ion beam from a discharge source with a given primary electron energy.

Ions might also undergo collisions with thermal electrons. Reference 3 also indicates that electron-ion recombination (arising primarily from three-body processes) with possible dissociation might occur with a frequency comparable to that for ionization.

Multiple ionization. - No evaluation of the degree of multiple ionization could be made in this program. Although multiple ionization can be reduced to a negligible level in a mercury discharge by operating at discharge voltages less than 50 volts (ref. 17), this may not be possible when a molecular compound is utilized, unless discharge voltages are quite near the molecular ionization potential.

Selection of Propellants

The following molecules were selected for testing: anthracene, pyrene, chrysene, 1,2,4,5-tetrabromobenzene, pentabromophenol, stannic iodide, selenium, and silicotungstic acid. The chemical formulas and atomic weights of these molecules are shown in table I.

Some of the molecular compounds were selected on a basis of expected stability to electron impact and desirable vapor pressure properties. A theoretical study (ref. 3) and references contained therein indicate that aromatic ring compounds would offer the best fragmentation resistance characteristics of any organic materials. Five molecules selected for testing were of this class. Three of these, pyrene, chrysene, and anthracene, are simple ring compounds to which heavy atoms might be attached to provide large, heavy molecules in future investigations. The other two molecules of this class, pentabromophenol and 1,2,4,5-tetrabromobenzene, are halogenated benzene ring compounds. As these compounds should be representative of the most stable organic materials under electron impact, no other organic types were investigated. Three inorganic materials, stannic iodide, selenium, and silicotungstic acid, were also investigated for two reasons: First, very little is known of the fragmentation patterns of inorganic materials, so for completeness it was felt that they should be tested in the program. Second, the three compounds selected represented a variety of intermolecular bonding types and initial molecular mass and hence might allow some comparison within inorganic compounds.

RESULTS AND DISCUSSION

The experimental results presented herein are divided into two categories. In the first section, data on the effective ion mass for the different propellants under investigation are compared at representative operating conditions for the electron-bombardment ion thrustor. In addition, thrustor performance data with the different propellants are shown. In the second section, the effect of altering various thrustor operating parameters on the effective ion mass of a single propellant, stannic iodide, is described.

Investigation of Different Selected Propellants

No data are presented for chrysene because no reliable measure of the neutral flow rate could be obtained during any test of this compound. Severe difficulties were encountered in controlling the neutral propellant flow rate when the electric vaporizer was utilized during tests of several compounds.

Also, no data are shown for silicotungstic acid for two reasons: First, during all tests with this compound, the discharge in the ion chamber quenched after a relatively short thrustor operating period. Inspection of the vaporizer, however, showed that most of the propellant remained unused. The measured neutral propellant flow rate agreed quite closely with the value to be expected from the loss of the waters of hydration for this compound. Second, the experimentally determined values for the effective ion mass were very close to the value to be expected for singly charged water molecules or oxygen. After the waters of hydration had apparently been removed from the propellant in the vaporizer, no ion beam could be obtained at vaporizer temperatures as high as 670° K.

Variation of effective ion mass with ion beam current. - Figure 4 shows the variation of effective ion mass, determined by thrust measurement, as a function of ion beam current for five propellants: stannic iodide, 1,2,4,5-tetrabromobenzene, anthracene, pentabromophenol, and selenium. Results for pyrene are not presented because data were not obtained for a range of ion beam current. The equivalent neutral beam current J_n varied over a large range during tests with the various propellants. It must be noted that the ion beam current does not specify the propellant utilization efficiency in the case of molecular propellants (eq. (2)).

The data show that the effective ion mass is much smaller than the parent ion mass over the entire range of ion beam current. With the exception of pentabromophenol and selenium, the effective ion mass of the propellants investigated remained fairly constant for values of ion beam current above about 0.05 ampere; however, as the ion beam current was decreased below 0.05 ampere, the effective ion mass tended to increase for all propellants, with the exception of 1,2,4,5-tetrabromobenzene. The effective ion mass for pentabromophenol and selenium increased nearly linearly with decreasing ion beam current.

The data for stannic iodide exhibit the largest calculated value for effective ion mass of all propellants studied. The effective ion mass for stannic iodide was about 140 atomic mass units at values of ion current above 0.05 ampere and increased sharply at lower values of ion beam current, becoming as large as 300 atomic mass units at about 0.01 ampere. During some tests with stannic iodide, ion beam currents as high as 3 times the neutral beam current were obtained for the assumption of a singly charged stannic iodide molecule. The results seem to indicate that many of the ions in the beam were singly charged iodide atoms.

The effective ion mass of 1,2,4,5-tetrabromobenzene is quite near the value for a singly charged bromine atom (80 amu). The composition of the ion beam cannot be specified from experimental thrust measurements because of the

complexity of the organic chemicals studied and because a given value for the effective ion mass may be produced from a variety of mass spectra. Additional data showed that values for ion beam current approximately as large as the equivalent neutral beam current could be obtained with 1,2,4,5-tetrabrobenzene. The ratio of effective beam ion mass to parent ion mass at this condition was approximately 1/5.

After all tests with 1,2,4,5-tetrabromobenzene, as was the case following most runs with the organic compounds, a black deposit was found on the screen, the anode, and the distributor plate. Chemical tests indicated that these deposits were carbon.

The effective ion mass for anthracene is nearly constant for values of ion beam current above 0.030 ampere but tends to increase as the ion beam current is lowered below 0.030 ampere. The highest value for the ion beam current that was obtained with anthracene was approximately equal to the equivalent neutral beam current.

The effective ion mass for pentabromophenol decreased linearly with increasing ion beam current for the range of ion beam current that was investigated. After pentabromophenol was investigated experimentally, data were found (ref. 16) which indicated that the compound dissociates on heating. Values for the ion beam current as high as 1.5 times the neutral beam current were obtained in one test with pentabromophenol.

The effective ion mass for selenium decreased slightly with increasing ion beam current for the range investigated and became approximately the value for the mass of a singly charged selenium atom (79 amu) as the ion beam current was increased above a value of 0.100 ampere. Values for the ion beam current as high as two times the neutral beam current were obtained for selenium for the assumption of a singly charged selenium molecule containing eight selenium atoms. Higher values for the ion beam current might have been attained were it not for space-charge limitations imposed by the accelerator grids. During this test, the electric vaporizer could not be controlled so that the data presented represents a very large variation in neutral propellant flow rates. Only one test was made because of the toxicity of selenium compounds.

Variation of effective ion mass with filament emission current. - Data presented in the previous section and all other data recorded at a constant ion beam current were taken by varying a given thrustor input parameter and adjusting the filament emission current to obtain the desired ion beam current. Since the filament emission current represents an important thrustor input parameter, the effect of filament emission current on the effective ion mass of the various propellants will now be shown.

Figures 5 and 6 show the effective ion mass of stannic iodide as a function of ion beam current and filament emission current, respectively, at three values of ion-chamber potential difference. It is seen that, within experimental error, the effective ion mass was affected primarily by the value of emission or beam current and not by the discharge voltage.

The similarity in the variations of effective ion mass with the emission and ion beam currents is a result of a linear relation between these two parameters in the range of mass utilization investigated. The variation of ion beam current with filament emission current, with all other thrustor variables held constant, is shown for stannic iodide in figure 7. The slope of this curve varied with each propellant.

Figures 8 to 10 show the variation in filament emission current necessary to maintain a constant ion beam current while varying ion-chamber potential difference, magnetic field intensity, or anode potential, respectively. The data in figures 8 and 10 were obtained with stannic iodide, and the data in figure 9 were obtained with 1,2,4,5-tetrabromobenzene; however, the results in these figures are representative for all propellants investigated. It is apparent from these figures that it was necessary to vary the filament emission current by a factor of about 2 in order to hold the ion beam current constant while varying each of the other thrustor input parameters over its operating range.

Attempts to separate the effects of the emission and ion beam currents were unsuccessful. Ion-molecule interactions in the ion beam should not be of primary importance in determining the ion mass spectra. The filament emission current, rather than the ion beam current, was then assumed to be the independent parameter in determing the effective ion mass.

Reference 18 contains data on the electron number density of a mercury discharge in an electron-bombardment thrustor. These data indicate that the ion-chamber discharge current (approx. equal to the filament emission current) influences both the thermal and primary electron number densities and that these densities are strong functions of axial and radial positions in the ionization chamber. Also, the thermal electron density was found to drop nearly an order of magnitude when the ion accelerating potentials were applied, while the radial density of primary electrons was less sensitive to variation of this thrustor parameter.

These data indicate the uncertainty in relating the filament emission current to plasma conditions, or to specific molecule and/or ion-electron interactions.

Variation of effective ion mass with ion-chamber potential difference. - The effect of ion-chamber potential difference on the effective ion mass of the heavy-molecular-weight propellants would appear important because the energy of ionizing electrons has a predominant influence on the mass spectra of molecular ions at electron energies near the ionization potential (ref. 14).

The data shown in figure 11 were obtained at constant values of ion beam current, magnetic field intensity, anode potential, accelerator potential, and neutral beam current for each propellant studied. The effective ion mass does not appear to be dependent on the ion-chamber potential difference over the range of stable thrustor operation. The greater part of the variation in effective ion mass, which was noted for most propellants, falls within the estimated experimental error (about ±20 percent) for the effective ion mass obtained from the experimental thrust measurements.

Figure 12 shows the effective ion mass of stannic iodide as a function of ion-chamber potential difference at two values of emission current. It is seen that a small increase in effective ion mass occurs as the discharge voltage decreases in value, however, the variation is less than 25 percent. Data of this type are limited by the large filament powers necessary to produce a constant emission current at low values of discharge voltage.

The range of ion-chamber potential difference over which the thrustor could be operated was limited by the following factors. At high values of ion-chamber potential difference (generally about 100 v), thrustor operation would become quite unstable, causing arcing and high-voltage breakdowns. At low values (16 to 20 v for most propellants), the ion-chamber discharge would be quenched, and no measurable ion beam current could be observed. The minimum value for the ion-chamber potential difference at which the discharge would be extinguished will be referred to as the quench potential for a particular propellant. The experimental values for the quench potential of most of the propellants tested are included in table I. Also listed are the ionization potential and the fragmentation potential when known (ref. 16). The quench potential is approximately twice the ionization potential for most of the propellants investigated.

It would be difficult to state specific reasons for the quenching of a molecular plasma. At values of electron energy approaching the ionization potential, however, the ionization cross sections of all the test compounds are greatly reduced, and various energy loss mechanisms (such as molecular excitation, bulk recombination, and ion withdrawal from the ionization chamber) might predominate and lead to quenching of the plasma. Such considerations indicate that it might be very difficult to produce a plasma, which is capable of supplying desired ion densities to the accelerator region, at discharge voltages near the molecular ionization potentials.

The inability to operate the thrustor at low values of discharge voltage precludes any conclusions, however, as to the significance of the primary electron energy in molecular fragmentation in the ionization chamber.

Variation of effective ion mass with magnetic field intensity. The effect of magnetic field intensity on the effective ion mass of anthracene and 1,2,4,5-tetrabromobenzene is shown in figure 13. The field was measured on the axis of the thrustor in the plane of the screen grid. Only the emission current was varied. The magnetic field intensity has a relatively small effect on the effective ion mass over the range investigated (21 to 64 gauss).

Variation of effective ion mass with anode potential. - The effect of anode potential on the effective ion mass for stannic iodide, 1,2,4,5-tetrabromobenzene, pentabromophenol, and pyrene is shown in figure 14. In general, the effective ion mass was nearly independent of anode potential. Although the effective ion mass of pentabromophenol and pyrene appear to increase with anode potential, the variation is within experimental error and is not considered conclusive. The data were recorded at a constant ratio of net to total accelerating voltage of 0.8 for all four propellants. In addition, the ion-chamber potential difference, the ion beam current, the magnetic field intensity, and the neutral beam current were held constant for each propellant.

Variation of effective ion mass with neutral beam current. - In order to vary the neutral number density in the discharge, neutral propellant flow rates were varied for three propellants, pentabromophenol, 1,2,4,5-tetrabromobenzene, and selenium.

Figure 15 shows the effective ion mass of 1,2,4,5-tetrabromobenzene as a function of ion current for two neutral flow rates, which differed by a factor of 1.5. These data were taken at constant anode voltage and magnetic field; however, the discharge voltage differed by 10 volts in the two tests. Figure 16 shows the effective ion mass as a function of ion-chamber potential difference for pentabromophenol for two flow rates, which differed by a factor of 4, while the ion currents varied by a factor of approximately 3.5. These data were taken at constant magnetic field and anode potential.

In both cases it is seen that the effective ion masses were slightly higher with increased neutral flow; however, as the data for each propellant were obtained in separate tests, comparisons are somewhat uncertain.

During the test with selenium, in which a very wide range of neutral beam currents was inadvertently obtained, no significant variation in effective ion mass was noted.

Thrustor efficiencies with selected propellants. - The most significant potential advantage in the use of heavy molecules as a propellant is in increased thrustor efficiency. It is of interest to show the effect of the various test propellants on thrustor performance. The results are discussed in the following order: propellant utilization efficiency, thrustor power efficiency, and overall thrustor efficiency.

Data presented in this report have shown that the effective ion mass of all the propellants studied is much lower than the parent mass. On the other hand, ion beam currents larger than the neutral beam current could be obtained for some of the propellants, which could be a result of either molecular fragmentation or multiple ionization. Figure 17 shows the normalized effective ion mass as a function of the normalized ion beam current. Lines of constant propellant utilization efficiency (which can be seen to be hyperbolas from eq. (2)) are also included in the figure. It is shown in figure 17 that the propellant utilization efficiency never exceeded 50 percent for any propellant studied. Operation of the thrustor at low levels of J_B/J_n (at which the higher values for the effective ion mass were obtained) resulted in a substantial reduction of the propellant utilization efficiency. In addition, it was generally necessary to operate at values of J_B/J_n greater than 1 to obtain propellant utilization efficiencies greater than 20 percent.

The thrustor power efficiency (ratio of beam power to power input) of the electron-bombardment thrustor was calculated in the same manner as described in reference 19. The variation of thrustor power efficiency with ion beam current is shown for stannic iodide in figure 18. Thrustor power efficiency tends to approach values of 60 to 70 percent as the ion beam current is increased. As the ion beam current is reduced to values below about 0.050 ampere, the thrustor power efficiency drops off sharply to values below 40 percent. These

data are representative for all propellants studied. It is evident, therefore, that the highest effective ion masses are obtained at the expense of low thrustor power efficiency.

The overall thrustor efficiency is the product of the propellant utilization efficiency and the thrustor power efficiency. The highest value obtained for overall thrustor efficiency was about 35 percent. Operation of the thrustor at conditions which lead to maximum values for the effective ion mass resulted in overall thrustor efficiencies of less than 10 percent for all propellants. For example, at an ion beam current of 0.020 ampere, the overall thrustor efficiency was about 4 percent for stannic iodide and about 8 percent for anthracene.

Variation of Thrustor Operating Parameters

The data of the previous sections indicate that production of ion beams of heavy molecules in a 10-centimeter-diameter electron-bombardment thrustor could be achieved only at extremely low levels of overall thrustor efficiency. Four sources of molecular fragmentation as well as multiple ionization were considered as possible explanations of the inability to obtain heavy molecular ions in quantity from a 10-centimeter-diameter electron-bombardment thrustor. Besides multiple ionization, these phenomena are fragmentation due to wall interactions, excessive neutral propellant temperature, excessive primary electron energy, and multiple ion and/or molecule-electron impact. A program of variation of both physical and electrical thrustor parameters was carried out to discover if any of these postulated difficulties could be identified and perhaps alleviated.

Stannic iodide was used for most of the tests for several reasons. It had the largest effective ion mass of any molecule tested, its structural simplicity might facilitate interpretation of the data, and lastly, a steam vaporizer could be utilized, which allowed more reliable measurements of the neutral propellant flow rates than did the use of an electric vaporizer.

Biased distributor plate. - A bias was applied to the distributor plate with respect to the filament and the screen to determine the effect of ions interacting with the surfaces of the ionization chamber. Three propellants were tested with the biased distributor: anthracene, 1,2,4,5-tetrabromobenzene, and pentabromophenol. The result of this variation is seen for 1,2,4,5-tetrabromobenzene in figure 19, where the bias is positive with respect to the screen. It is seen that the positive bias voltage had little effect on the effective ion mass. Additional data, not plotted, indicated that negative bias voltages (to 20 v) also produced no variation in effective ion mass for 1,2,4,5-tetrabromobenzene. With anthracene and pentabromophenol no variation in thrust was recorded over a 0- to +60-volt range of distributor bias for either molecule.

The complexity of plasma interactions makes it difficult to estimate the degree to which biasing the distributor plate would affect ion-wall interactions. Ion-wall collisions could occur at the screen, the anode, the outer chamber surface, and the filament regardless of the distributor bias. The

effect of ions striking the filament is probably small, however, since the ratio of filament to ionization chamber surfaces is usually about 0.01. In addition, fields in the discharge chamber (ref. 11) and near the acceleration region (ref. 10) would be such to reduce ion-wall interactions at the anode and the screen, respectively. Such considerations then indicate that the distributor plate would be a major source of ion-wall interactions. The fact that the effective ion mass was not dependent upon distributor bias does indicate that ion-wall interactions are probably not a primary source of fragmentation in the discharge.

Variation of filament emitting area. - As shown previously, it was impossible to obtain measurable beam currents at discharge voltages near the ionization potential of any of the molecules. The data in table I show that, in most cases, the minimum operating potential was about twice the ionization potential, where data allowed direct comparison.

Several types of filaments were tested in a 10-centimeter-diameter thrustor with stannic iodide to determine whether an increase in the emitting area of the filament would allow lower discharge voltages to be utilized. Two tantalum filaments, one a ribbon design and the other a single wire, that differed in surface area by a factor of 9 were tested under otherwise almost identical thrustor conditions. The neutral propellant flows differed by 15 percent. There was no effect, within experimental error, in the minimum operating voltages that could be achieved, and no substantial difference was noted in the effective ion masses obtained with the two filaments. The quench potentials in these tests were measured and found to be about 3 volts lower for the filament with the smaller emitting area. For any molecule during a given test, quench potentials would vary by as much as 2 volts, so that such measurements must be considered somewhat inconclusive. Filaments with the same ratio of emitting areas were tested in a 10-centimeter-diameter thrustor with a 2.5-centimeter-long ionization chamber with similar results. Neither the quench potentials nor the effective ion mass seemed to be affected by the filament emitting area.

Thrustor operation with a barium oxide coated cathode (ref. 20) proved unsuccessful, as the propellant, stannic iodide, apparently poisoned the cathode.

Variation of neutral density. - The effect of increased neutral density was investigated utilizing a 5-centimeter-diameter thrustor. The neutral propellant flow rate of stannic iodide was approximately the same as that for the tests with the 10-centimeter-diameter thrustor. In two tests with the small thrustor, the quench potentials were 18 and 20 volts, which compare with the 17- and 20-volt quench potentials of the 10-centimeter-diameter thrustor. The effective ion masses measured were very similar to those obtained with the 10-centimeter-diameter thrustor.

Variation of ionization chamber length. - In order to reduce the number of molecular and/or ion-electron collisions within the ionization chamber, an attempt was made to decrease the molecular residence time.

Ionization chamber lengths of 9.2, 5, and 2.5 centimeters were tested with stannic iodide as the propellant. Shortening the ionization chamber also

served to reduce the area available for ion-wall interactions.

Figure 20 shows the effective ion mass for the three chamber lengths as a function of thrustor ion current. Two strands of 0.025-centimeter-diameter tantalum wire were used as a filament in the 9.2-centimeter-long ionization chamber, while ribbon filaments were utilized in the other two tests. The neutral propellant flow rates were equal within about 10 percent. It is seen that the ionization chamber length had little effect on the effective ion mass of stannic iodide.

Several difficulties were experienced in testing the thrustor with the 2.5-centimeter-long ionization chamber. Quite often, the discharge would quench as the net accelerating potential was increased. Quench potentials were very high with this thrustor configuration. During calibration tests with mercury, the minimum voltage at which the thrustor could be operated was more than twice the quench potentials for mercury recorded when the two longer ionization chambers were used. Also, during the calibration tests, it was noted that the use of the short ionization chamber limited the maximum achievable propellant utilization efficiency to about 60 percent. Over 95 percent utilization efficiency could be obtained in the other chamber configurations with mercury.

The operational difficulties incurred with the short chamber indicate that further shortening of the ionization chamber would not allow a discharge to occur. In addition, the frequent quenching of the discharge when the accelerating potentials were increased might indicate that it would be difficult to ionize required quantities of molecules by electron bombardment in a strong ion withdrawal field. The reductions in propellant utilization efficiencies resulting from use of a short ionization chamber indicate that it may not be possible to combine efficient ionization with short molecular residence times without substantial losses in thrustor efficiency.

Variation of propellant feed. - A side-feed electron-bombardment thrustor (unpublished data obtained by Paul D. Reader of Lewis) was also used in order to affect the molecular residence times. This thrustor differs in design from all others tested in that the propellant is introduced into the ionization chamber approximately radially from the anode surface between 2.5 and 5 centimeters from the upstream face of the screen. The results of this test are shown in figure 21. It is seen that the effective ions mass decreased linearly with the ion current. The results at low ion currents are similar to most other tests with stannic iodide.

As no significant improvements in the effective ion mass were noted with any of the thrustor geometric or electrical variations, the overall thrustor efficiencies were not substantially different from those found in the first phase of the study.

CONCLUDING REMARKS

The results of this investigation indicate that an electron-bombardment thrustor of the type presently used for ionization of atomic species cannot be

utilized to obtain heavy molecular ions in quantity at acceptable levels of thrustor efficiency.

As no molecule had an effective ion mass greater than one-half the mass of the parent ion, no useful comparison of the test propellants could be made on a basis of molecular composition or interbonding type.

Variation of a number of operational parameters in a 10-centimeter-diameter electron-bombardment thrustor indicated that only the filament emission current strongly affected the effective ion mass of the ion beam over the levels of thrustor parameters investigated. Because of the complicated interrelation between emission current and plasma conditions, however, no attempt was made to describe this dependence in terms of specific molecular interactions.

Variation of a number of thrustor parameters had no significant effect on the effective ion mass of the thrustor ion beam. Attempts to reduce the discharge voltage at which ion beams could be produced, by varying filament emitting area and increasing the density of neutrals in the ionization chamber, were unsuccessful. The fact that the effective ion mass is not dependent upon the distributor plate bias and ionization chamber surface area indicates that ion-wall interactions are not of primary importance in the determination of the ion beam mass spectra. The attempt to reduce the residence times of the molecular and ionic species, both by shortening the ionization chamber and by introducing the propellant near the screen, led to no significant improvement in effective ion mass and, in the case of the shortest ionization chamber, led to large reductions of thrustor efficiency.

Experiments did indicate, however, that molecule and/or ion interactions with primary electrons are the major factor in the molecular fragmentation process. The complicated relation between the various thrustor parameters and the molecular plasma, the relatively crude measuring technique, and the inability to influence to a significant extent the effective ion mass with variations in thrustor electrical and geometric parameters (with the exception of filament emission current) precluded exact identification of the primary causes of molecular fragmentation.

Lewis Research Center
National Aeronautics and Space Administration
Cleveland, Ohio, April 30, 1964

APPENDIX A

SYMBOLS

B magnetic field intensity, gauss

C constant, $1.44 \times 10^{-4} \frac{\text{newton}}{\text{amp}\sqrt{\text{amu}}\sqrt{\text{v}}}$

F thrust, newtons

J current, amp

L ionization chamber length, cm

M mass, amu

V potential, v

ΔV potential difference, v

Y sputtering yield, atoms/ion

η_u propellant utilization efficiency

Subscripts:

A accelerator

B ion beam

E emission

F filament

I anode

m effective ion

mag magnet

n neutral beam

p parent

s index

SD screen-distributor

APPENDIX B

THRUST TARGET

The thrust targets used in the experiment were fabricated of either stainless steel or titanium sheet 0.025 and 0.05 millimeter thick, respectively. They were suspended by four 0.125-millimeter-diameter tantalum wires that were approximately 58 centimeters long. The masses of both the titanium and stainless steel targets were approximately 70 grams. The targets were hung by centering the cone on the longitudinal axis of the thrustor.

Initially, an electric transducer was used to record thrust target deflection. Many difficulties were experienced with this measuring technique. An optical cathetometer was then used to measure the target movement, and use of this device reduced experimental "down time" and provided more reliable results. All data presented in this report were taken with the optical cathetometer.

Analysis of Data

In this section a brief analysis is given to delineate the significance of the data taken with the thrust target.

The total thrust of an ion beam is, in the case of a single ion species,

$$F = C\sqrt{V_I}\, J_B \sqrt{M}$$

The particle mass, which may be calculated from a thrust measurement and which will be referred to as the effective ion mass, is

$$M_m = \frac{F^2}{C^2 V_I J_B^2} \tag{B1}$$

In the case of fragmentation, however, when single ionization is assumed, the thrust of an ion beam is

$$F = C\sqrt{V_I} \sum_s J_s \sqrt{M_s} \tag{B2}$$

where J_s is the ion current in amperes associated with a particular ion fragment of mass M_s in atomic mass units. The index s ranges over all values of M_s present in the ion beam. The effective ion mass is

$$M_m = \left(\sum_s J_s \sqrt{M_s} \sum_s J_s \right)^2 \tag{B3}$$

since

$$J_B = \sum_s J_s \tag{B4}$$

When the fragmentation exists, the ion mass, calculated from a thrust measurement, is the square of the average square root of the ion masses. It can be shown that the measured effective ion mass is equal to or less than the mean mass of the ionized fragments in the thrustor ion beam. It will be assumed, however, for purposes of calculation of mass utilization efficiencies, that the effective ion mass is equal to the mean mass of the fragment ions. This approximation is probably adequate. For example, calculating a mean mass and an effective ion mass from a mass spectrum of anthracene (ref. 3) resulted in a difference of only 5 percent.

Calibration Techniques

A mercury ion beam was used to calibrate the thrust target for most tests. The thrustor, with geometric conditions exactly like those to be used in the following heavy-molecule tests, was operated over a variety of beam levels and impulses.

It was assumed that the mercury ion beam represents a known thrust. Care was taken to reduce multiple ionization by operating at discharge voltages less than 50 volts. A curve of thrust as a function of target deflection may then be obtained with the mercury beam as a known thrust. Quite linear and repeatable results were obtained with this method. Figure 22 shows a typical calibration curve. In most calibration curves, two regions of nonlinearity were noted. At large beam currents, always greater than 100 milliamperes, there appears to be considerable beam divergence, although the current at which this sets in is quite dependent on the net accelerating potential. Nonlinearities also appear at low beam currents, usually less than 15 milliamperes. At small thrust levels errors in the data such as leakage currents, meter unreliabilities, and error in measuring the deflection could become quite significant in the thrust calculation.

The mercury beam calibration then provided a linear repeatable calibration over a large range of beam currents. It is believed that such a target allows a direct comparison of thrusts between a mercury and a heavy-molecule ion beam.

While the mercury ion beam calibration should allow a good comparison of thrust it is of interest to evaluate the accuracy of this calibration technique in providing reliable absolute thrust measurements.

A pulley arrangement was used to determine absolute calibration curves. A number of weights were attached by a string to the target and suspended over a pulley. The friction forces were roughly measured and found to be negligible when compared with the weights used in the calibration. This method provides a direct measurement of deflection as a function of thrust. Figure 22 shows such a curve taken with the same thrust target used for the mercury ion beam

calibration curve of that figure. It is seen that the two calibration techniques gave quite similar results in the linear region of the beam calibration.

The use of simple pendulum equations provides another method for obtaining an absolute calibration (ref. 10). An estimate can be made of the effective length of the cone pendulum either by measuring the vertical suspension or period of oscillation of the thrust target. A curve of thrust as a function of deflection can then be calculated. Because of the long facility shutdown cycle necessary to obtain an accurate measurement of the period and the uncertainty in the significance of a direct measurement of the vertical suspension distance, the pulley system was used to determine the absolute thrust calibration.

Errors in Thrust Measurement

Three sources of error in the thrust measurement are beam spreading, sputtering phenomena, and inaccuracies in use of the optical cathetometer.

Beam spreading. - Data were taken with an impingement current probe (ref. 21) to determine the degree of beam spreading. These data indicated that, in the range of ion currents used in this program, the amount of the ion beam striking the thrust target was at least 97 percent of the total ion current.

Sputtering phenomena. - An attempt was made to estimate the effect of sputtering on the thrust measurement by both a rough theoretical calculation and an experimental measurement.

In order to determine the thrust that sputtered titanium might produce, it is necessary to estimate both the sputtering yield Y (atoms/ion) and the energy of the sputtered ions. From an extrapolation of the data of reference 22 concerning the energy of sputtered tungsten atoms due to incident singly charged mercury ions of kinetic energies up to 900 electron volts, it is estimated that the maximum energy of sputtered titanium atoms would be approximately 50 electron volts at incident ion energies of about 4000 volts.

It is difficult to estimate the yield for the experimental situation. The angle of incidence is 15°, and it will be assumed that ion bombardment at this angle will increase the yield by a factor of 2 over normal incidence (ref. 23). Although no data were available for the case of titanium sputtered by mercury ions in the energy range of interest, data from reference 9 led to the approximation that $Y = 2$. A calculation of the thrust from sputtered particles follows.

The ratio of the thrusts from the mercury ions to the sputtered titanium on a per ion basis is then taken to be, from equation (1),

$$\left.\begin{aligned} \frac{F_{Hg}}{F_{Ti}} &= \frac{C\sqrt{V_{Hg}}\, J_{Hg}\sqrt{M_{Hg}}}{C\sqrt{V_{Ti}}\, J_{Ti}\sqrt{M_{Ti}}} \\ \text{or} \\ \frac{F_{Hg}}{F_{Ti}} &= \frac{C}{C}\,\frac{\sqrt{4000}}{\sqrt{50}}\,\frac{1}{2}\,\frac{\sqrt{200}}{\sqrt{48}} \\ \text{and} \\ \frac{F_{Hg}}{F_{Ti}} &= 9 \end{aligned}\right\} \qquad \text{(B5)}$$

so that the thrust from sputtered particles would represent at most one-ninth of the total thrust. A rough one-dimensional analysis indicates that less than one-half of the sputtered atoms escapes the target, so that the total effect of sputtering on the thrust measurement was estimated to be less than 5 percent.

A measurement of the weight loss of the thrust target over a period of testing was made to assess the sputtering loss in the thrust target. It was found that the weight loss corresponded to an average current of 20 milliamperes of titanium atoms. If the energy is taken to be 50 electron volts, this loss corresponds to a thrust of approximately 0.03 millipound, which is about one-tenth of the smallest thrust at which data were recorded.

Error in optical cathetometer measurements. - Tests were carried out with the optical cathetometer, and measurements were found to be repeatable to within about 5 percent at the lowest levels of thrust target deflection at which data were taken.

Total error in calculation of effective ion mass. - The preceding considerations indicate that an error of approximately 10 percent is the maximum to be expected in the thrust measurement. Since the experimental thrust is squared in calculation of the effective ion mass, it is concluded that the error in the values of effective ion mass should usually be less than 20 percent.

REFERENCES

1. Mickelsen, William R.: Comparative Performance of Electrostatic Rocket Engines. Paper 62-74, IAS, 1962.

2. Kaufman, H. R.: The Electron-Bombardment Ion Rocket. Paper Presented at AFOSR Symposium on Advanced Propulsion Concepts, Cincinnati (Ohio), Oct. 2-4, 1962.

3. Dugan, John V., Jr.: Some Theoretical Bases for Selection of Molecular Ion Propellants and a Survey of Molecular Plasma Collision Processes. NASA TN D-1185, 1964.

4. Reader, Paul D.: Investigation of a 10-Centimeter-Diameter Electron-Bombardment Ion Rocket. NASA TN D-1163, 1962.

5. Nakanishi, Shigeo, Pawlik, Eugene V., and Baur, Charles W.: Experimental Evaluation of Steady-State Control Properties of an Electron-Bombardment Ion Thrustor. NASA TN D-2171, 1964.

6. Pawlik, Eugene V., and Wenger, Norman C.: Performance Evaluation of a Mercury-Propellant Feed System for a Flight-Model Ion Engine. NASA TN D-1213, 1962.

7. Kerslake, William R.: Accelerator Grid Tests on an Electron-Bombardment Ion Rocket. NASA TN D-1168, 1962.

8. Dushman, Saul: Scientific Foundations of Vacuum Technique. John Wiley & Sons, Inc., 1958.

9. Almen, O., and Bruce, G.: High Energy Sputtering. 1961 Trans. of Eighth Vacuum Symposium and Second Int. Cong., Pergamon Press, 1962, p. 245.

10. Kerslake, William R., and Pawlik, Eugene V.: Additional Studies of Screen and Accelerator Grids for Electron-Bombardment Ion Thrustors. NASA TN D-1411, 1963.

11. Domitz, Stanley: Experimental Evaluation of a Direct-Current Low-Pressure Plasma Source. NASA TN D-1659, 1963.

12. Cottrell, T. L.: The Strengths of Chemical Bonds. Second ed., Butterworths Sci. Pub., 1958, pp. 173-235.

13. Wallace, Rita J., Hopper, W. L., Garrett, Barry B., and Anderson, R. C.: Exploratory Experiments on Surface Deposits on Metals from Pyrolysis of Hydrocarbons. Tech. Note 7, Texas Univ., Dec. 1961.

14. Stevenson, D. P., and Schissler, D. O.: Mass Spectrometry and Radiation Chemistry. The Chemical and Biological Action of Radiations, Vol. V, Academic Press, Inc., 1961, pp. 217-241.

15. Milder, Nelson L., and Kerslake, William R.: Evaluation of Filament Deterioration in Electron-Bombardment Ion Sources. NASA TN D-2173, 1963.

16. Anon.: Propellants for Electrical Propulsion Engines of the Contact or Bombardment Ion Type. R-3556, Second Annual (Final) Rep. Mar. 15, 1961 - Mar. 15, 1962, Rocketdyne, Nov. 16, 1962.

17. Milder, Nelson L.: Comparative Measurements of Singly and Doubly Ionized Mercury Produced by Electron-Bombardment Ion Engine. NASA TN D-1219, 1962.

18. Strickfaden, William B., and Geiler, Kenneth L.: Probe Measurements of the Discharge in an Operating Electron-Bombardment Engine. TR 32-417, Jet Prop. Lab., C.I.T., Apr. 19, 1963.

19. Kaufman, Harold R.: An Ion Rocket with an Electron-Bombardment Ion Source. NASA TN D-585, 1961.

20. Beck, A. H. W.: High-Current-Density Thermionic Emitters: A Survey Proc. Instit. Electrical Eng., pt. B, vol. 106, no. 28, July 1959, pp. 372-388; discussion, pp. 389-390.

21. Reader, Paul D., and Finke, Robert C.: An Electron-Bombardment Ion Rocket Operated with Alternating-Current Supplies. NASA TN D-1457, 1962.

22. Wehner, G. K.: Velocities of Sputtered Atoms. Phys. Rev., vol. 114, no. 5, June 1, 1959, pp. 1270-1272.

23. Wehner, Gottfried K.: Influence of the Angle of Incidence on Sputtering Yields. Jour. Appl. Phys., vol. 30, no. 11, Nov. 1959, pp. 1762-1765.

TABLE I. - HEAVY MOLECULE DATA

Molecule	Formula	Atomic mass, amu	Experimental quench potential, v	Ionization potential, v (a)	Fragmentation potential, v (a)	Experimental vapor pressure at 100° C, mm Hg
Anthracene	$C_{14}H_{10}$	178	16	8.41	12.3	2×10^{-1}
Pyrene	$C_{16}H_{10}$	202	(b)	8.8	(b)	10^{-2}
Chrysene	$C_{18}H_{12}$	228	(b)	7.71	16	10^{-3}
1,2,4,5-Tetrabromobenzene	$C_6H_2Br_4$	394	16 to 18	10.7	15	5×10^{-2}
Pentabromophenol	C_6Br_5OH	489	20	(b)	(b)	3×10^{-3}
Stannic iodide	SnI_4	626	17 to 21	(b)	(b)	(b)
Selenium	Se_8	632	(b)	(b)	(b)	2×10^{-6}
Silicotungstic acid	$H_4SiW_{12}O_{40}\cdot 24H_2O$	3311	34	(b)	(b)	(b)

[a]Data from ref. 16.

[b]No data available.

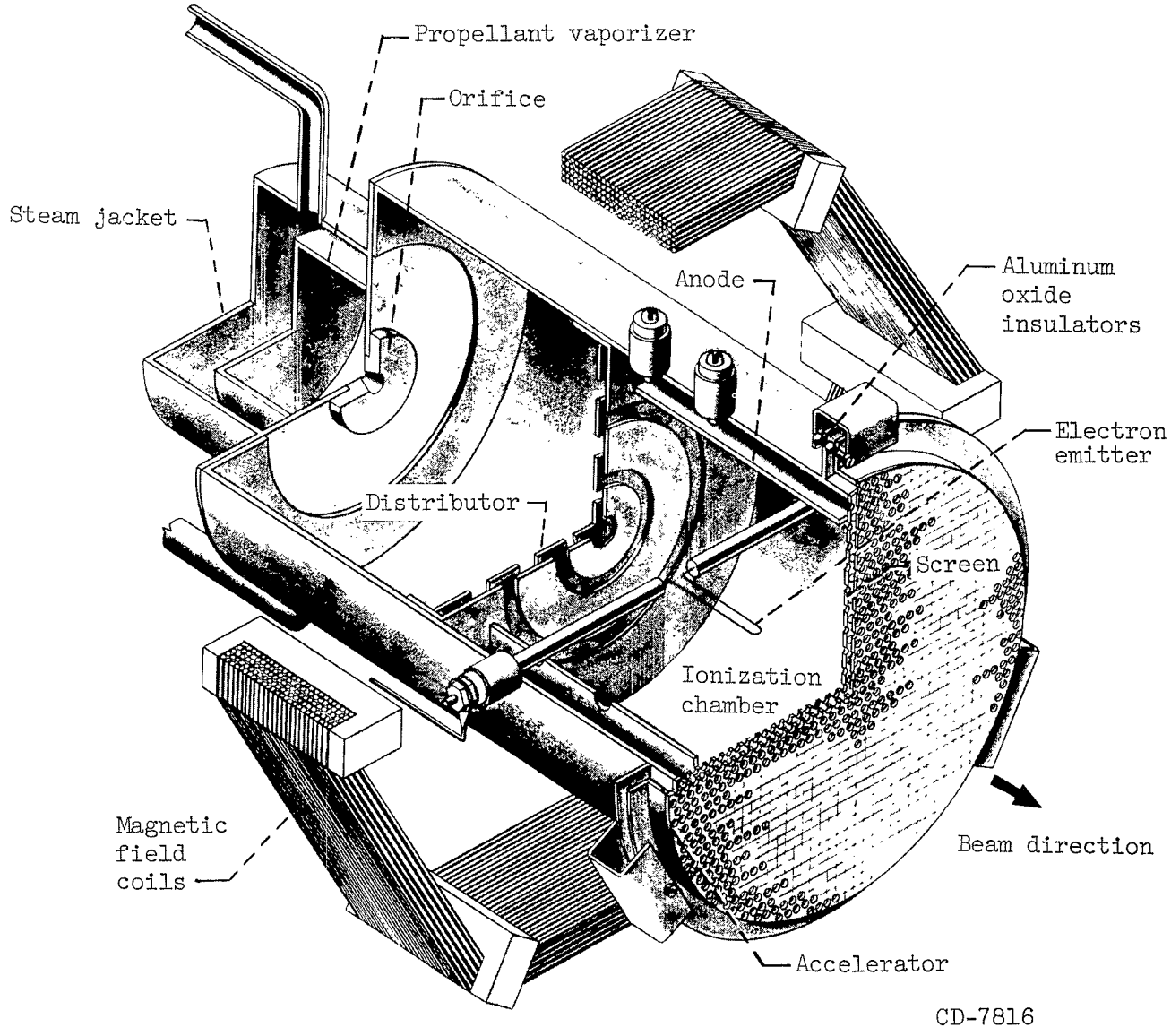

Figure 1. - Cutaway sketch of 10-centimeter-diameter electron-bombardment thrustor.

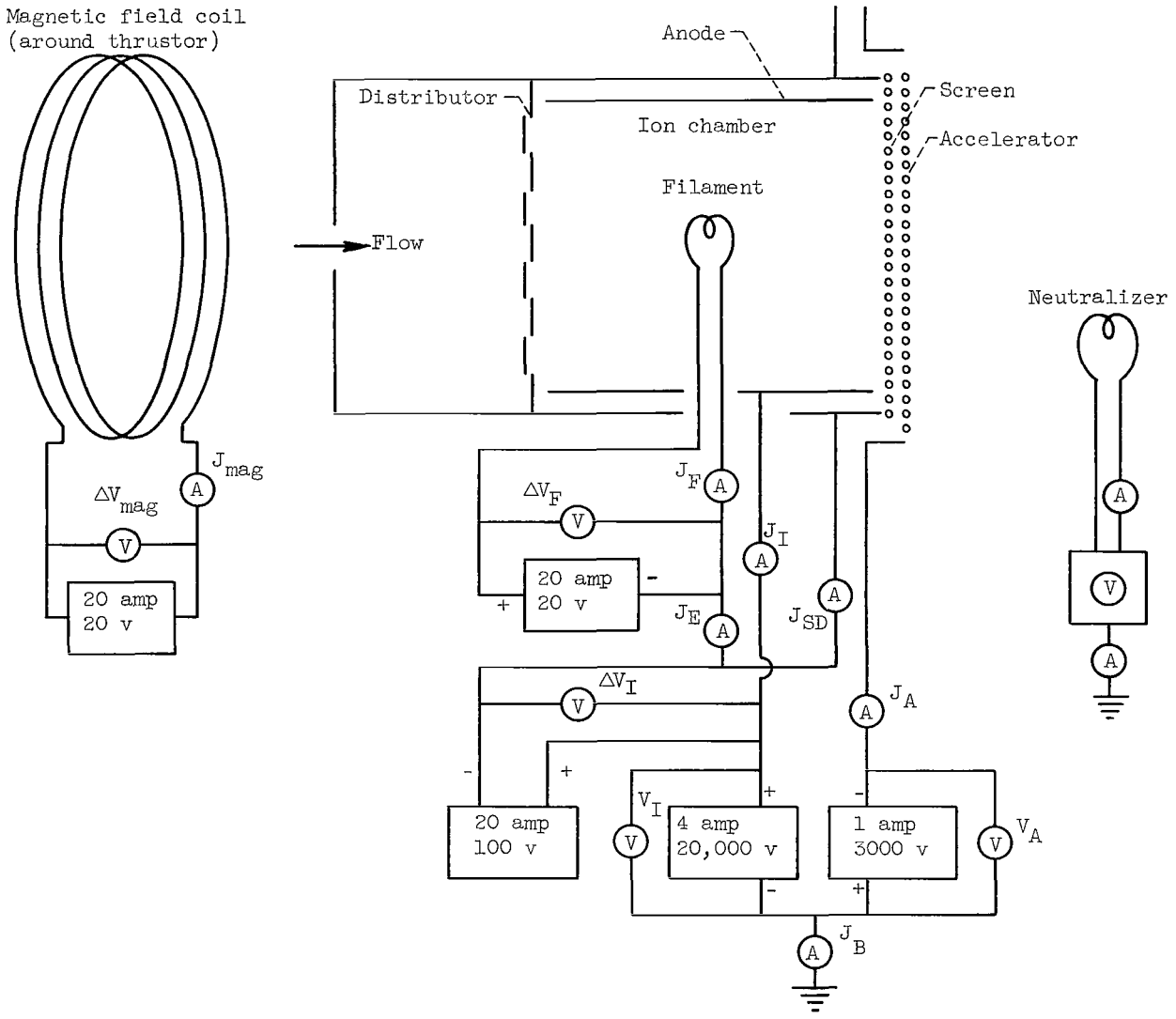

Figure 2. - Wiring diagram of ion thrustor.

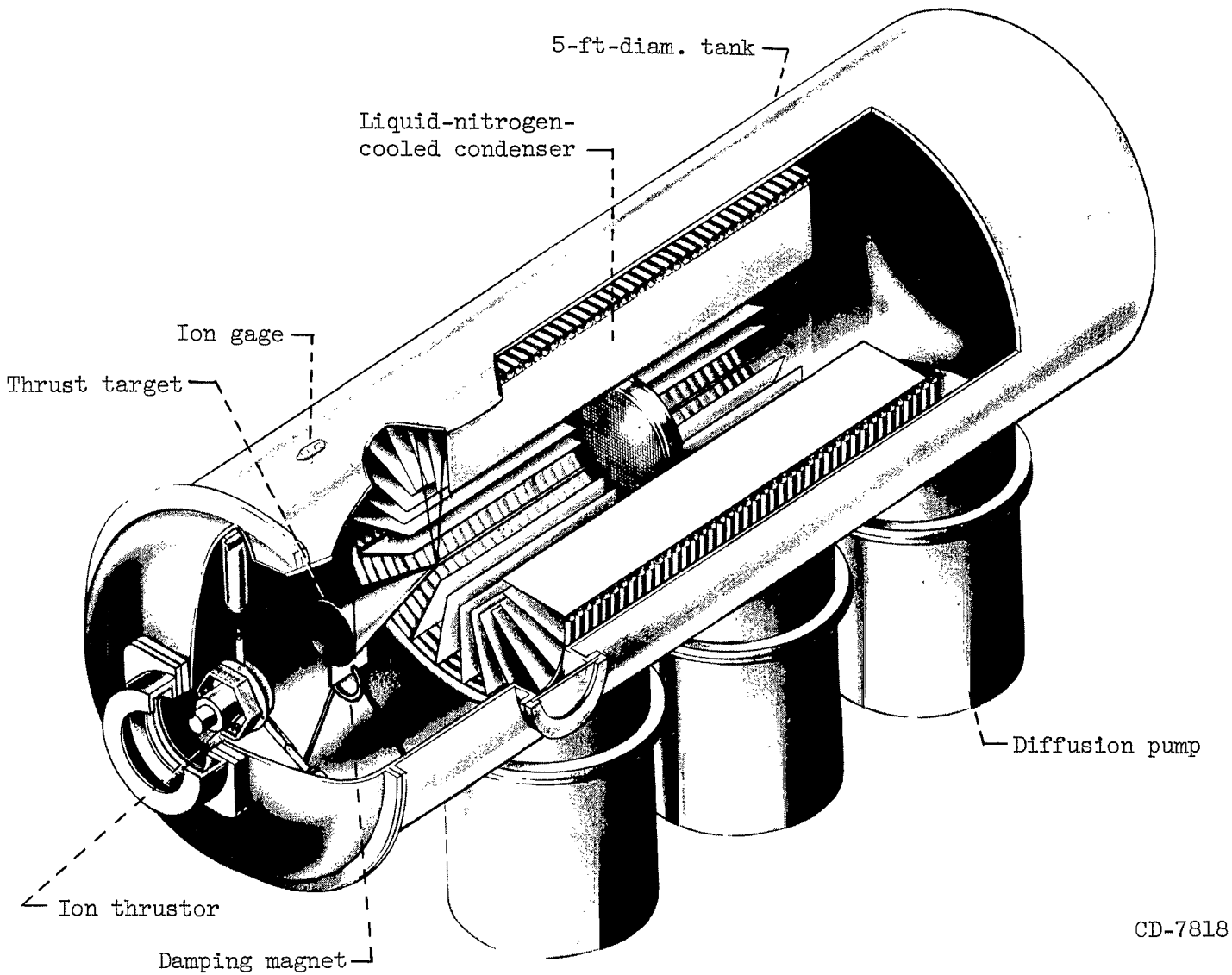

Figure 3. - Thrustor and thrust target positions in vacuum tank.

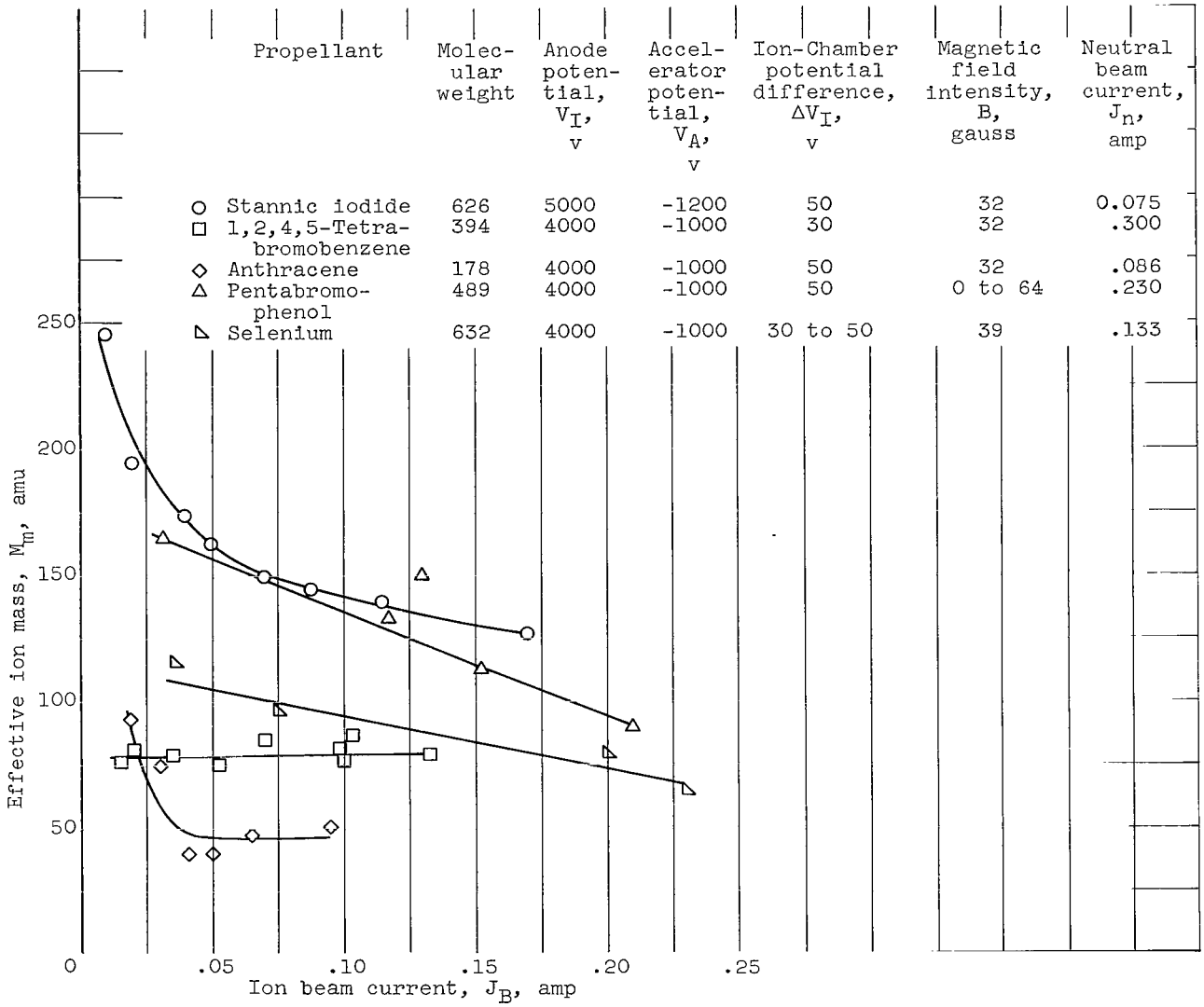

Figure 4. - Variation of effective ion mass with ion beam current for five propellants.

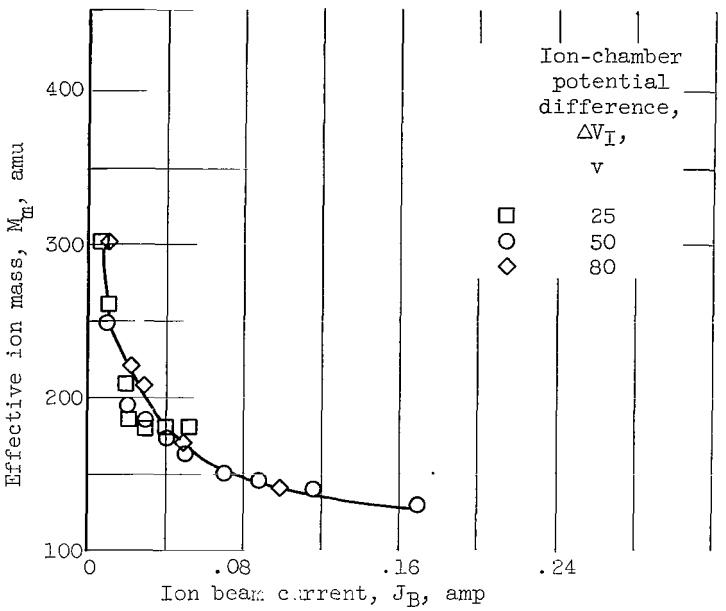

Figure 5. - Variation of effective ion mass with ion beam current for three values of ion-chamber potential difference. Propellant, stannic iodide; anode potential, 5000 volts; accelerator potential, -1250 volts; magnetic field intensity, 32 gauss; neutral beam current, 0.075 ampere.

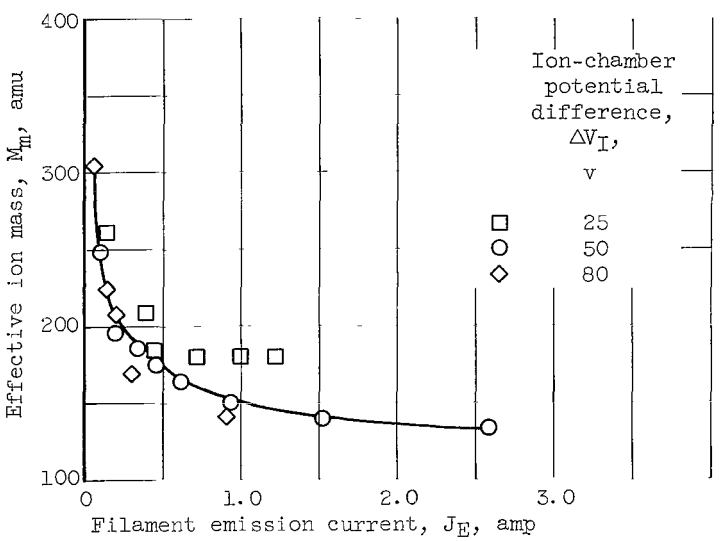

Figure 6. - Variation of effective ion mass with filament emission current for three values of ion-chamber potential difference. Propellant, stannic iodide; anode potential, 5000 volts; accelerator potential, -1250 volts; magnetic field intensity, 32 gauss; neutral beam current, 0.075 ampere.

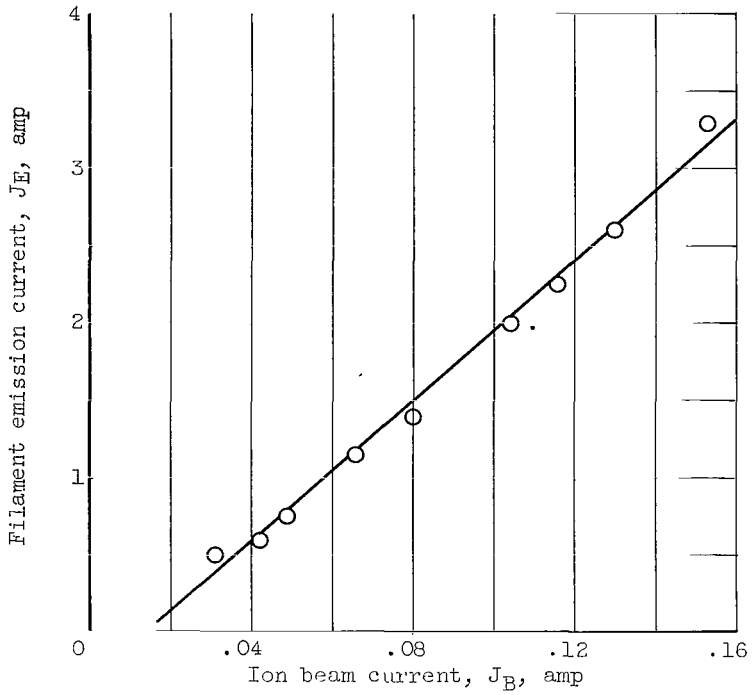

Figure 7. - Variation of ion beam current with filament emission current. Propellant, stannic iodide; anode potential, 4000 volts; accelerator potential, -1000 volts; magnetic field intensity, 32 gauss; neutral beam current, 0.072 ampere; ion-chamber potential difference, 50 volts.

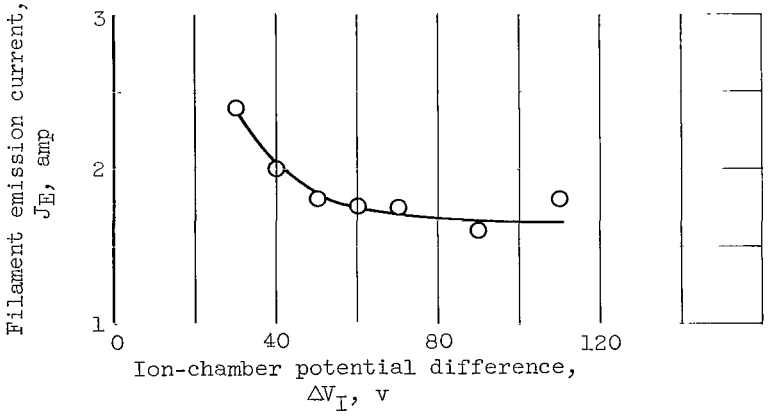

Figure 8. - Effect of ion-chamber potential difference on filament emission current. Propellant, stannic iodide; anode potential, 4000 volts; accelerator potential, -1000 volts; magnetic field intensity, 32 gauss; neutral beam current, 0.072; ion beam current, 0.100 ampere.

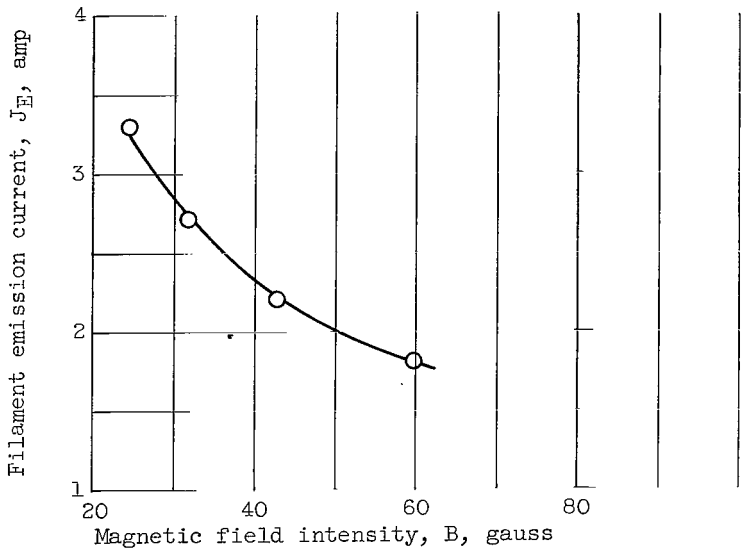

Figure 9. - Effect of magnetic field intensity on filament emission current. Propellant, 1,2,4,5-tetrabromobenzene; anode potential, 4000 volts; accelerator potential, -1000 volts; neutral beam current, 0.300 ampere; ion-chamber potential difference, 30 volts; ion beam current, 0.095 ampere.

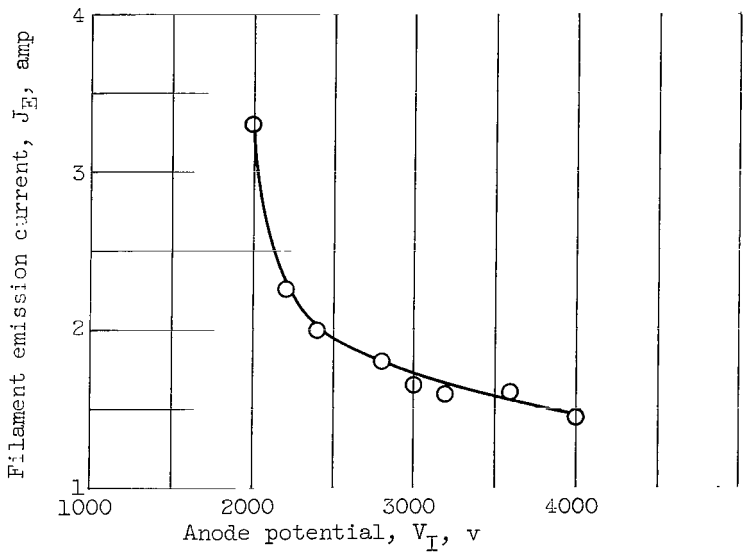

Figure 10. - Effect of anode potential on filament emission current. Propellant, stannic iodide; magnetic field intensity, 32 gauss; neutral beam current, 0.072 ampere; ion chamber potential difference, 50 volts; ion beam current, 0.087 ampere; ratio of net to total accelerating voltage, 0.8.

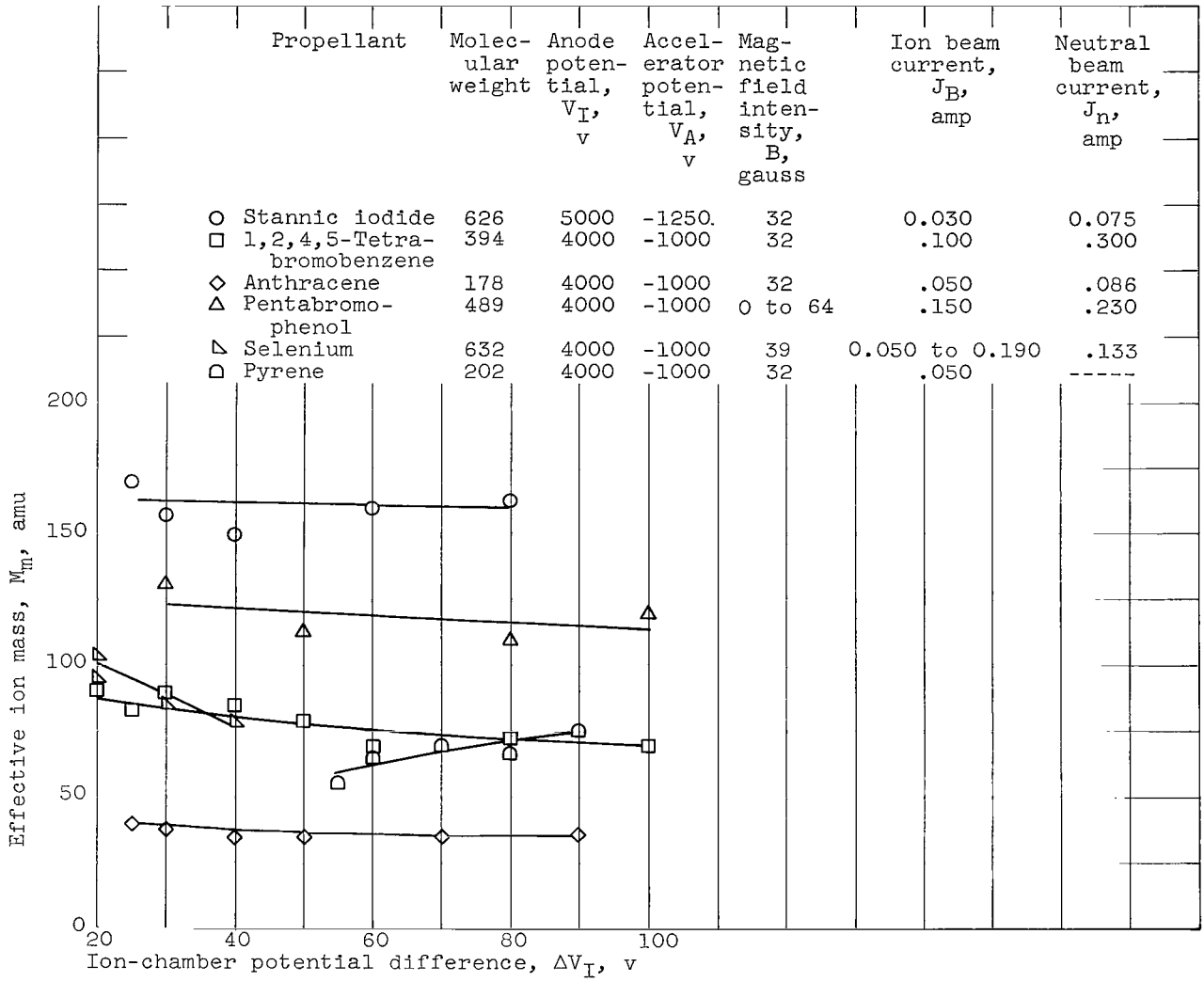

Figure 11. - Variation of effective ion mass with ion-chamber potential difference for six propellants.

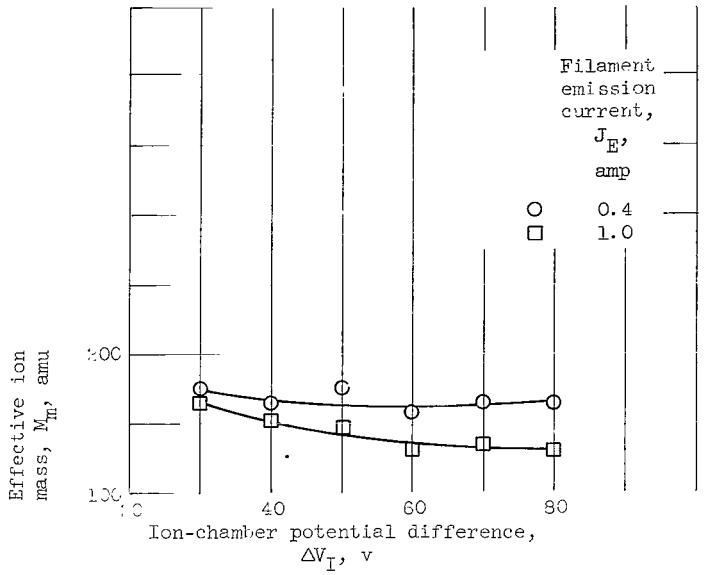

Figure 12. - Variation of effective ion mass with ion-chamber potential difference for two values of filament emission current. Propellant, stannic iodide; anode potential, 5000 volts; accelerator potential, -1250 volts; magnetic field intensity, 32 gauss; neutral beam current, 0.075 ampere. Ion beam current, 0.023 to 0.048 ampere and 0.050 to 0.060 ampere at filament-emission-current values of 0.4 and 1 ampere, respectively.

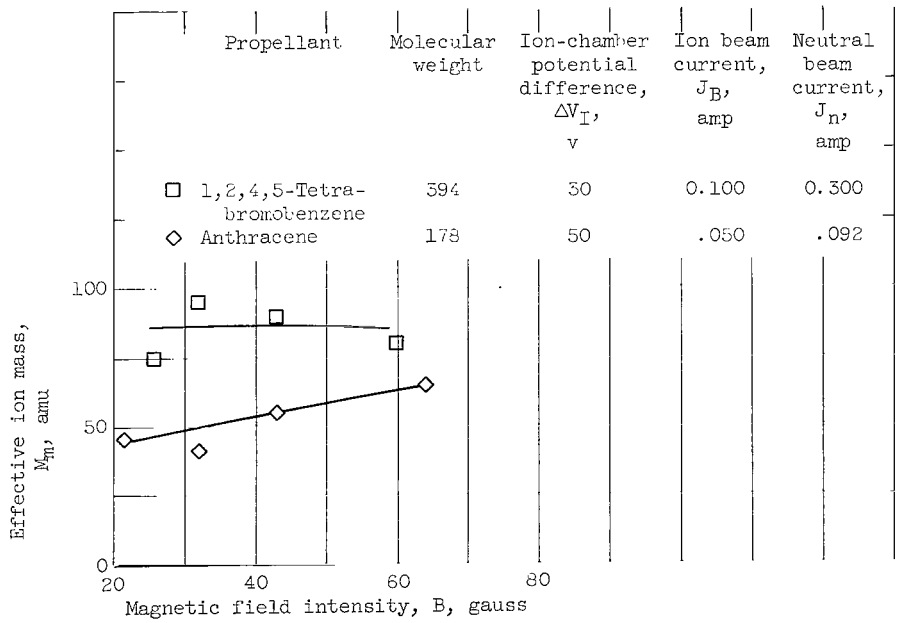

Figure 13. - Variation of effective ion mass with magnetic field intensity for 1,2,4,5-tetrabromobenzene and anthracene. Anode potential, 4000 volts; accelerator potential, -1000 volts.

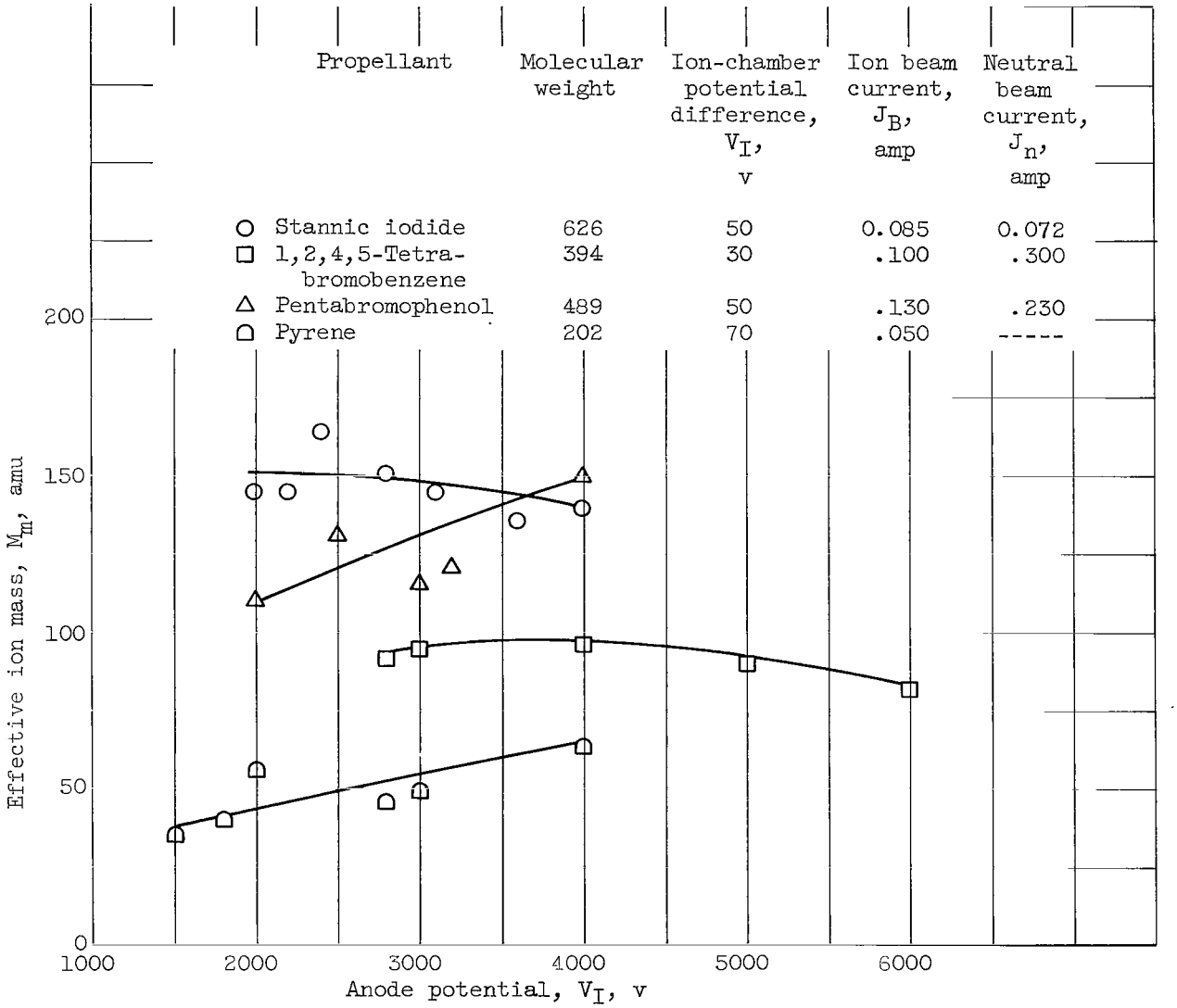

Figure 14. - Variation of effective ion mass with anode potential (net accelerating potential) for four propellants. Magnetic field intensity, 32 gauss; ratio of net to total accelerating voltage, 0.8.

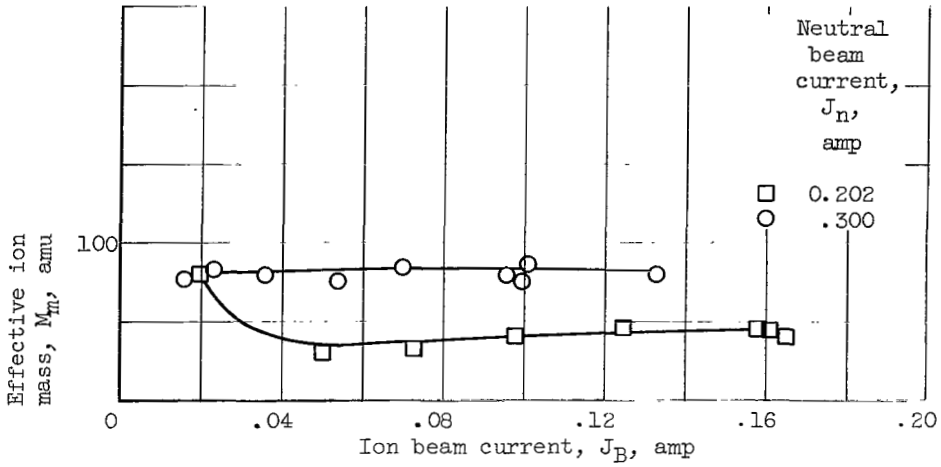

Figure 15. - Variation of effective ion mass with ion beam current for two values of neutral beam current. Propellant, 1,2,4,5-tetrabromobenzene; anode potential, 4000 volts; accelerator potential, -1000 volts; magnetic field intensity, 32 gauss; ion-chamber potential difference, 40 and 30 volts at neutral-beam-current values of 0.202 and 0.300 ampere, respectively.

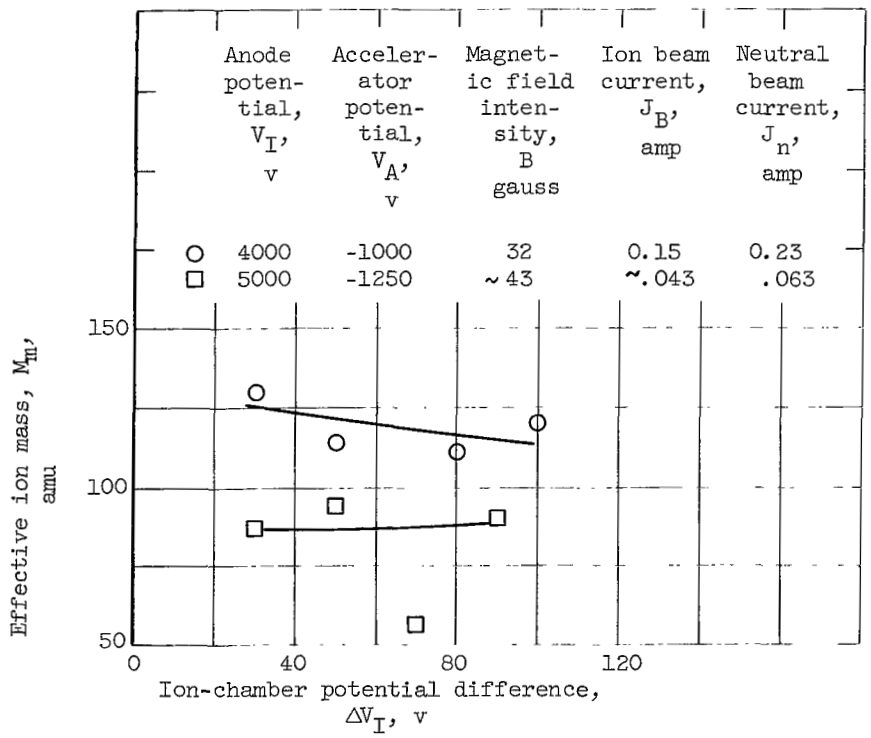

Figure 16. - Variation of effective ion mass with ion-chamber potential difference for pentabromophenol at two values of neutral beam current.

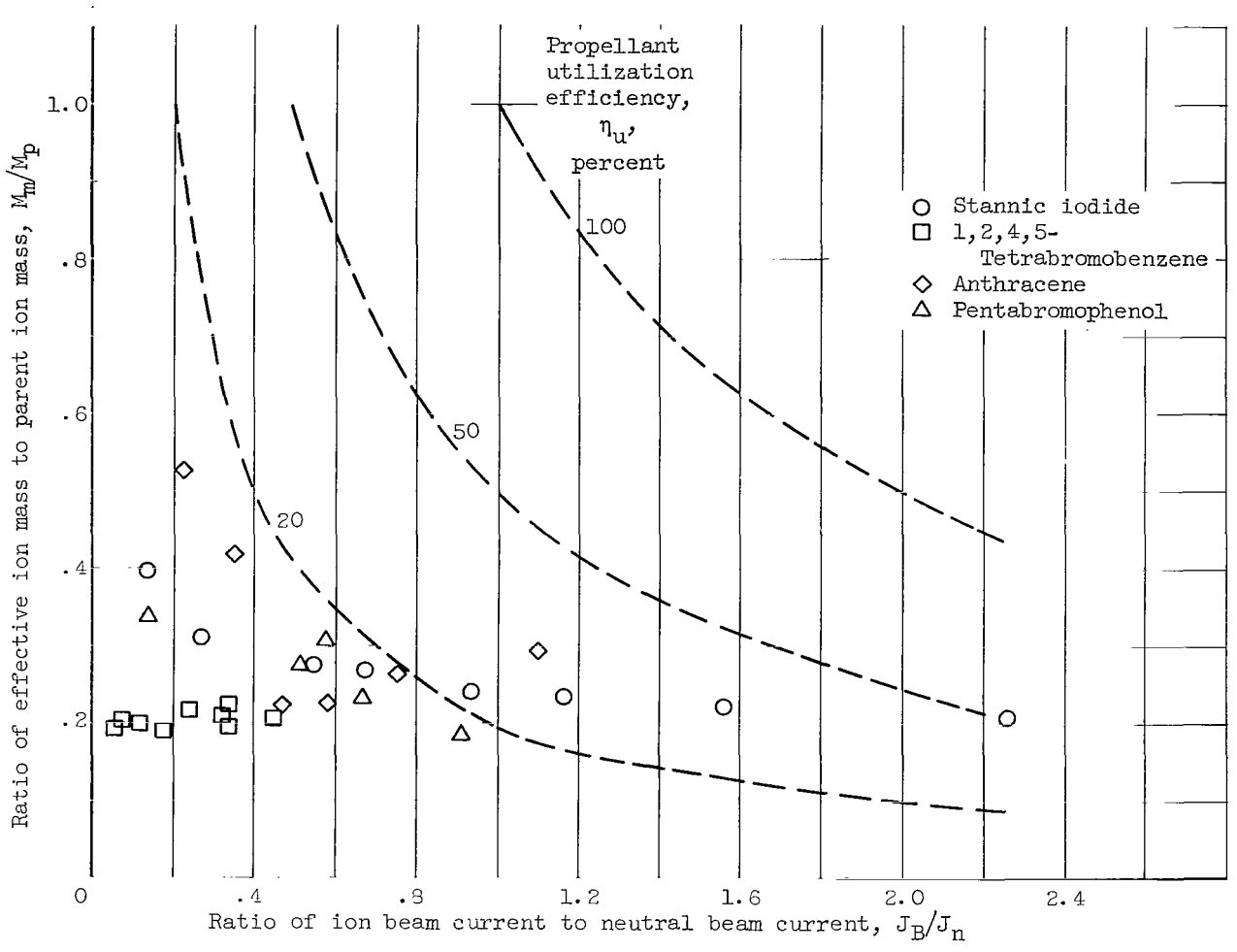

Figure 17. - Normalized effective ion mass as function of normalized ion beam current (data of fig. 4).

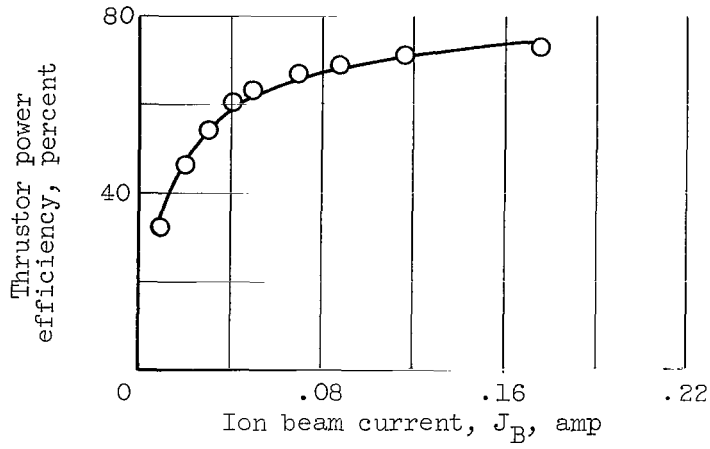

Figure 18. - Variation of thrustor power efficiency with ion beam current. Propellant, stannic iodide; anode potential, 5000 volts; accelerator potential, -1250 volts; magnetic field intensity, 32 gauss; neutral beam current, 0.072 ampere; ion-chamber potential difference, 50 volts.

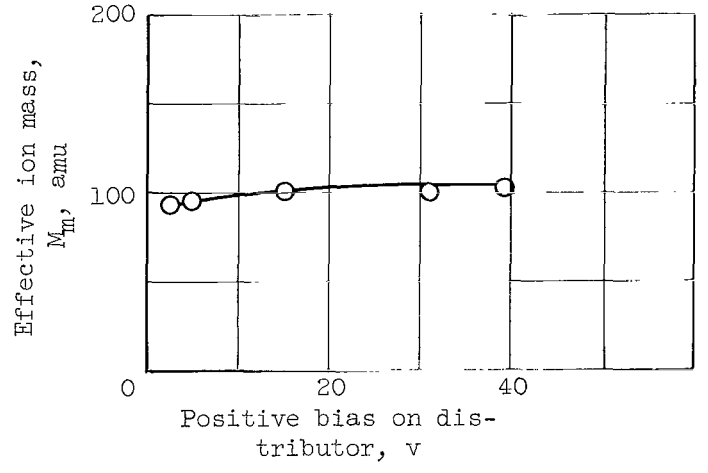

Figure 19. - Variation of effective ion mass with positive bias on distributor. Propellant, 1,2,4,5-tetrabromobenzene; anode potential, 4000 volts; accelerator potential, -1000 volts; magnetic field intensity, 32 gauss; neutral beam current, 0.300 ampere; ion-chamber potential difference, 30 volts; ion beam current, 0.100 ampere.

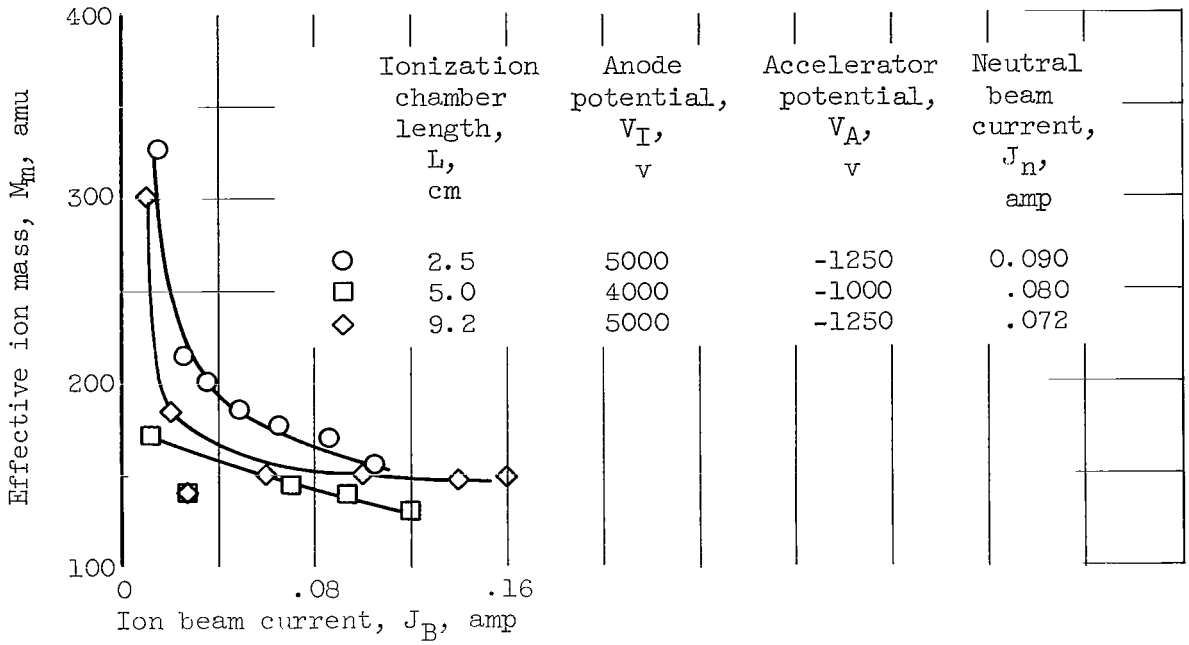

Figure 20. - Variation of effective ion mass with ion beam current for three ionization chamber lengths in 10-centimeter-diameter electron-bombardment thrustor. Propellant, stannic iodide; magnetic field intensity, 32 gauss; ion-chamber potential difference, 30 volts.

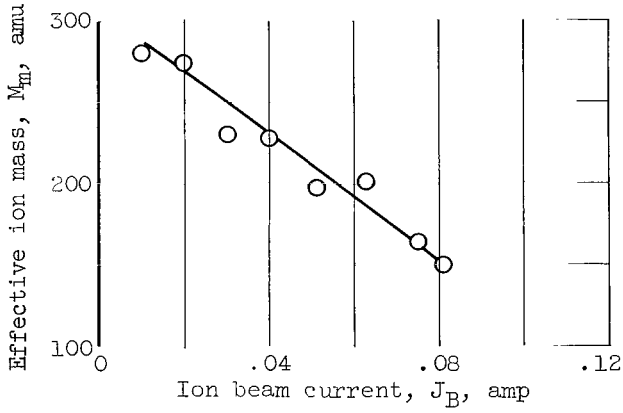

Figure 21. - Variation of effective ion mass with ion beam current in side-propellant-feed 10-centimeter-diameter electron bombardment thrustor. Propellant, stannic iodide; anode potential, 4000 volts; accelerator potential, -1000 volts; magnetic field intensity, 32 gauss; neutral beam current, 0.075 ampere; ion-chamber potential difference, 50 volts.

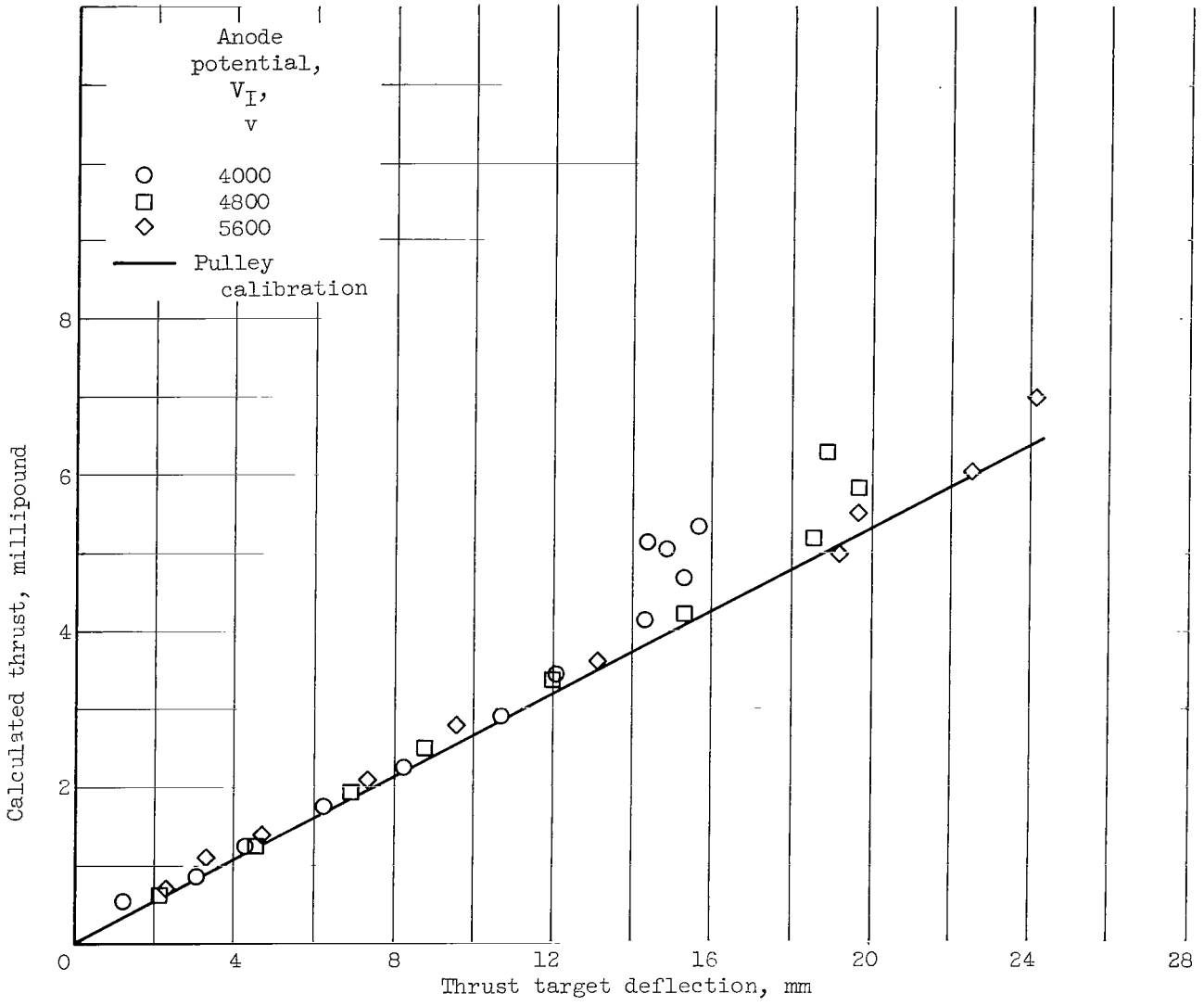

Figure 22. - Mercury thrust target calibration. Calculated thrust as function of target deflection. Ratio of net to total accelerating voltage, 0.8.

2/7/85

"The aeronautical and space activities of the United States shall be conducted so as to contribute . . . to the expansion of human knowledge of phenomena in the atmosphere and space. The Administration shall provide for the widest practicable and appropriate dissemination of information concerning its activities and the results thereof."

—NATIONAL AERONAUTICS AND SPACE ACT OF 1958

NASA SCIENTIFIC AND TECHNICAL PUBLICATIONS

TECHNICAL REPORTS: Scientific and technical information considered important, complete, and a lasting contribution to existing knowledge.

TECHNICAL NOTES: Information less broad in scope but nevertheless of importance as a contribution to existing knowledge.

TECHNICAL MEMORANDUMS: Information receiving limited distribution because of preliminary data, security classification, or other reasons.

CONTRACTOR REPORTS: Technical information generated in connection with a NASA contract or grant and released under NASA auspices.

TECHNICAL TRANSLATIONS: Information published in a foreign language considered to merit NASA distribution in English.

TECHNICAL REPRINTS: Information derived from NASA activities and initially published in the form of journal articles.

SPECIAL PUBLICATIONS: Information derived from or of value to NASA activities but not necessarily reporting the results of individual NASA-programmed scientific efforts. Publications include conference proceedings, monographs, data compilations, handbooks, sourcebooks, and special bibliographies.

Details on the availability of these publications may be obtained from:

SCIENTIFIC AND TECHNICAL INFORMATION DIVISION

NATIONAL AERONAUTICS AND SPACE ADMINISTRATION

Washington, D.C. 20546